Assessing an Energy-Based Control for the Soft Inverted Pendulum in Hamiltonian Form

Giulia Pagnanelli, *Graduate Student Member, IEEE*, Michele Pierallini, *Graduate Student Member, IEEE*, Franco Angelini, *Member, IEEE*, and Antonio Bicchi, *Fellow, IEEE*

***Abstract*—Thanks to their continuously deformable structure, continuum soft robots are suited for safe human-robot interactions. However, the executable tasks are still limited in complexity due to the high number of degrees of freedom, and the consequent under-actuation that characterizes these robots complicates the control problem. To develop a control strategy taking advantage of the main system properties this letter investigates the use of Interconnection and Damping Assignment Passivity Based Control in the regulation of unstable equilibria of the under-actuated template model *soft inverted pendulum* with affine curvature. We show that remarkably, the partial differential equations that arise from the application of this technique, have a closed-form solution for this system. We verify the effectiveness of the controller via simulations, and we compare the results achieved considering the swing-up problem against the ones obtained with baseline controllers, i.e., Proportional Derivative control and Feedback Linearization.**

***Index Terms*—Control applications, robotics, stability of nonlinear systems.**

I. Introduction

In RECENT years, soft robots have been the subject of many studies to guarantee safety and comfort in human-robot interactions [1]. Inspired by nature, the aim of soft robotics is to reproduce the behavior of animal muscles which, thanks to elasticity and compliance, allows the execution of many interesting tasks.

In the last years, many hardware solutions have been developed by exploiting several mathematical models, materials, and actuation [2], [3]. However, the tasks that can be executed are limited in complexity due to control problems. The high number of Degrees of Freedom (DoFs) that characterize the deformable structure and the consequent under-actuation are the main reasons for control difficulties. Consequently, model-free approaches have spread widely in the soft robotic field [4], as they allow the development of complex and efficient control without perfectly knowing the structure. Despite the simplicity of developing a dynamic control with the model-free approach, practical applications are limited by time and stability problems.

To date, the main challenge is to develop a model-based control strategy to take advantage of the behavior and characteristics of continuum soft robots. This letter focuses on the *Soft Inverted Pendulum (SIP)* (Fig. 1) presented in [5] and proposes a model-based control strategy designed to target the energetic components of the system, closely intertwined with the elastic elements. These components are pivotal in shaping the dynamics of the considered robot class and endow the system with intrinsic intelligence.

In [5] Collocated and Non-Collocated Feedback Linearization controls are proposed without considering the energy characteristics of the system. However, since energy covers the main role in the dynamic behavior one possibility is to develop an *energy based control* [6], i.e., Passivity Based Control (PBC). The PBC consists of controlling a system to make the closed-loop system passive. In terms of energy, PBC is an extension of the *energy-shaping* plus *damping injection* methodology. The energy-shape act allows the modification of the potential energy in such a way the new one has a global minimum at the equilibrium. The damping injection act modifies the dissipation properties of the system to make it passive guaranteeing stability. In the case of PBC, the energy shaping allows rendering the closed-loop system passive, characterized by a new desired storage function. This function is composed of the original kinetic energy of the system and the new desired potential energy. The damping injection reinforces this procedure to make the output strictly passive. However, applying this method to under-actuated systems destroys the Euler-Lagrange structure. This means that the storage function does not have the physical meaning of energy. The solution is the *Interconnection and Damping Assignment-Passivity Based Control (IDA-PBC)* [7], which is different from PBC that first selects a storage function and

Manuscript received 12 February 2024; revised 19 April 2024; accepted 10 May 2024. Date of publication 24 May 2024; date of current version 12 June 2024. This work was supported in part by the EU Horizon 2020 Research and Innovation Programmes: Project NI: "Natural Intelligence for Robotic Monitoring of Habitats" under Grant 101016970; in part by the Ministry of University and Research (MUR) as a part of the PON 2014-2021 "Research and Innovation" Resources–Green/Innovation Action under Grant DM MUR 1062/2021; in part by the Italian Ministry of Education and Research (MIUR) in the framework of the FoReLab Project (Departments of Excellence); and in part by the European Union by the Next Generation EU Project Ecosistema dell'Innovazione' Tuscany Health Ecosystem (THE, PNRR, Spoke 4: Spoke 9: Robotics and Automation for Health) under Grant ECS00000017. Recommended by Senior Editor L. Menini. *(Corresponding author: Giulia Pagnanelli.)*

Giulia Pagnanelli, Michele Pierallini, and Franco Angelini are with the Centro di Ricerca "Enrico Piaggio" and the Dipartimento di Ingegneria dell'Informazione, Universita di Pisa, 56126 Pisa, Italy (e-mail: giulia.pagnanelli17@gmail.com).

Antonio Bicchi is with the Centro di Ricerca "Enrico Piaggio" and the Dipartimento di Ingegneria dell'Informazione, Universita di Pisa, 56126 Pisa, Italy, and also with the Soft Robotics for Human Cooperation and Rehabilitation, Fondazione Istituto Italiano di Tecnologia, 16163 Genoa, Italy.

Digital Object Identifier 10.1109/LCSYS.2024.3405410

© 2024 The Authors. This work is licensed under a Creative Commons Attribution-NonCommercial-NoDerivatives 4.0 License.
For more information, see https://creativecommons.org/licenses/by-nc-nd/4.0/

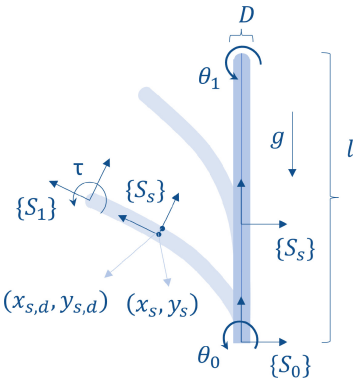

Fig. 1. Model of the SIP showing key parameters: gravity g, actuation with a pure torque τ, length l, diameter D. Configuration variables θ_0 and θ_1 are the weights of the affine function that describes the robot's curvature.

then designs a controller to render the storage function non-increasing, because the control action is divided in *energy shaping action* to assign desired energy function to the passive map, and *damping injection* to have asymptotic stability of the equilibrium in closed-loop. This control strategy requires the definition of the Hamiltonian equation [8] of the system and the modification of both kinetic and potential energy. Moreover, the main challenge to the applicability of the method is the resolution of Partial Differential Equations (PDEs) to derive the control law.

Recently, in [9], a PBC application has been presented for a general class of continuum soft robots without the damping assignment because of the difficulties involved in solving PDEs. An IDA-PBC is formulated in [10], [11] for a rigid link model with elastic joints but does not include the gravitational energy in the Hamiltonian function because their systems present a negligible mass. The present study contributes to the field of continuum soft robotics by:

- formulating an IDA-PBC control for the SIP: unlike previous approaches that assume negligible mass, our formulation includes gravitational energy, making it suitable for systems where mass cannot be ignored;
- deriving closed-form solutions for PDEs: we demonstrate the existence of closed-form solutions for the PDEs governing the soft inverted pendulum model. This enables the definition of energy-based control strategies, allowing efficient control implementation;
- investigating stability with varying stiffness: we explore how the stability of the controlled continuum soft robot varies with changes in stiffness. This analysis provides insights into the robustness and adaptability of the proposed control method under different mechanical conditions.

Simulation results are presented to prove that the proposed method allows the stabilization of the robot on its unstable vertical configuration, countering the natural behavior of the robot. Then, to show the competitiveness of the energy-based control, we provide a comparison with a *Proportional-Derivative (PD)* and a *Feedback Linearization (FL)* already presented in the literature [3], [5].

II. Problem Definition

A. Background

The detailed description of the SIP template problem can be found in [5]. Here, we summarize briefly its main points.

The overall shape of the robot is described by the configuration of the robot's central axis. In turn, this is univocally specified at each point by the curvature function, which is

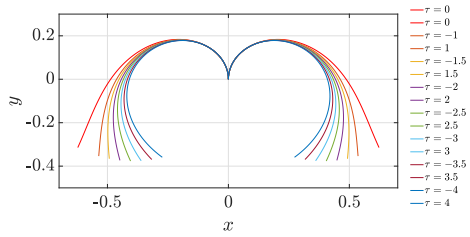

(a) Equilibria of the SIP evaluated for $k = 1$.

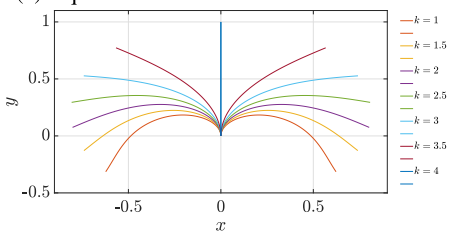

(b) Equilibria of the SIP evaluated for $\tau = 0$.

Fig. 2. Graphical representation of the bifurcation of equilibria obtained when varying (a) the input with stiffness equal to 1; and (b) the stiffness with zero input.

assumed affine $\kappa_s(t) = \theta_0(t) + \theta_1(t)s$ [5]. Here, θ_0 and θ_1 are the constant and linear components of κ and serve as configuration variables. t is the time variable and $s \in [0, 1]$ is the coordinate to parameterize the positions along the main axis of the pendulum. Let us define as $d \in [-\frac{1}{2}, \frac{1}{2}]$ the coordinate to parametrize points within the segment, thus a generic point (s, d) can be defined with coordinates $(x_{s,d}, y_{s,d})$ in the global frame (Fig. 1). The SIP dynamics is defined as follows [5]

$$B(\theta)\ddot{\theta} + C(\theta, \dot{\theta})\dot{\theta} + G(\theta) + kH\theta + \beta H\dot{\theta} = H\begin{bmatrix}1\\0\end{bmatrix}\tau, \quad (1)$$

where $\theta = [\theta_0, \theta_1]^\top$, $\dot{\theta}$, and $\ddot{\theta} \in \mathbb{R}^2$ are the position, velocity, and acceleration vectors, respectively, $B(\theta) \in \mathbb{R}^{2\times2}$ is the inertial matrix, $C(\theta, \dot{\theta}) \in \mathbb{R}^{2\times2}$ is Coriolis matrix, $G(\theta) \in \mathbb{R}^2$ is the gravity vector, $k \in \mathbb{R}$ is the robot stiffness, $\beta \in \mathbb{R}$ is the damping and $\tau \in \mathbb{R}$ is the input, which is a pure torque applied on the robot tip. $H \in \mathbb{R}^{2\times2}$ is the Hankel matrix whose elements are defined as $H_{i,j} = \frac{1}{i+j-1}$; note that it is full rank. Imposing the equilibrium conditions $\dot{\theta} = [0, 0]^\top$ and $\ddot{\theta} = [0, 0]^\top$ in (1) leads to

$$G_1(\bar{\theta}) + k\bar{\theta}_0 + \frac{k}{2}\bar{\theta}_1 = \bar{\tau}, \quad G_2(\bar{\theta}) + \frac{k}{2}\bar{\theta}_0 + \frac{k}{3}\bar{\theta}_1 = \frac{\bar{\tau}}{2}. \quad (2)$$

with $\bar{\theta}$ equilibrium configuration and $\bar{\tau}$ the equilibrium torque. Since $G(0, 0) = [0, 0]^\top$, the configuration $\theta = [0, 0]^\top$ is an equilibrium for $\bar{\tau} = 0$, and its stability depends on the stiffness value in relation to mass m and length l. If the stiffness is such that

$$\frac{k}{lgm} > \frac{13 + 2\sqrt{31}}{60}, \quad (3)$$

the equilibrium is stable [5]. On the other hand, if $\theta \neq [0, 0]^\top$ a closed-form solution for (2) does not exist. Fig. 2 reports some equilibria that are numerically evaluated varying τ (Fig. 2(a)) and k (Fig. 2(b)), respectively.

The dynamics of the SIP model (1) can be reformulated in Hamiltonian form using standard procedures documented in the literature [12]. This formulation is suitable for the definition of an energy-based control law. By adopting the more commonly used mathematical notation for clarity, we

define $q \triangleq \theta$, and $p \triangleq B(q)\dot{q}$ and then express the Hamiltonian (total energy) of the SIP as

$$\mathscr{H}(q,p) = \frac{1}{2}p^\top B^{-1}(q)p + \frac{k}{2}q^\top Hq + mgh\,. \tag{4}$$

The first term in (4) is the kinetic energy of the pendulum, and the remaining two are the elastic and gravitational potential energy, respectively. Therefore, our system in the Hamiltonian form [8] is

$$\begin{bmatrix}\dot{q}\\ \dot{p}\end{bmatrix} = \left(\underbrace{\begin{bmatrix}0 & I\\ -I & 0\end{bmatrix}}_{J(q,p)} - \underbrace{\begin{bmatrix}0 & 0\\ 0 & \beta H\end{bmatrix}}_{R(q,p)}\right)\begin{bmatrix}\nabla_q\mathscr{H}\\ \nabla_p\mathscr{H}\end{bmatrix} + \begin{bmatrix}0\\ A\end{bmatrix}u, \tag{5}$$

where $\nabla_q(\cdot) \triangleq \frac{\partial(\cdot)}{\partial q}$ and $\nabla_p(\cdot) \triangleq \frac{\partial(\cdot)}{\partial p}$ are the vectors of partial derivatives with respect to p and q, $u \in \mathbb{R}$ is the control input, $I \in \mathbb{R}^{2\times 2}$ identity matrix, H is the Hankel matrix, $\beta \in \mathbb{R}$ is the natural damping of the system, and $A = [1,\ \frac{1}{2}]^\top$. $J(q,p)$ and $R(q,p)$ are defined as the interconnection and damping matrix, respectively.

B. Problem Statement

Let us consider the case for which the vertical configuration $\theta^* = [0,0]^\top$ is an unstable equilibrium, i.e., when the stiffness k does not satisfy (3). The goal of this letter is to stabilize the SIP in this unstable configuration, i.e., the swing-up problem, by designing a passivity-based control.

III. Problem Solution

In this section, we show that the challenge introduced in Section II-B can be solved by opportunely defining the SIP model in the Hamiltonian, taking into account the gravitational contribution because the mass is not negligible, and opportunely defining the IDA-PBC showing that resulting PDEs admit solution.

Applying IDA-PBC means designing the control law in such a way the closed-loop is still in the Hamiltonian form and resulting as in [13]

$$\begin{bmatrix}\dot{q}\\ \dot{p}\end{bmatrix} = \big[J_\mathrm{d}(q,p) - R_\mathrm{d}(q,p)\big]\begin{bmatrix}\nabla_q\mathscr{H}_\mathrm{d}\\ \nabla_p\mathscr{H}_\mathrm{d}\end{bmatrix}, \tag{6}$$

where $J_\mathrm{d} = -J_\mathrm{d}^\top$ is the desired interconnection matrix, $R_\mathrm{d} = R_\mathrm{d}^\top$ is the desired damping matrix, and $\mathscr{H}_\mathrm{d}$ is the new Hamiltonian function. We choose

$$\mathscr{H}_\mathrm{d}(q,p) = \frac{1}{2}p^\top B_\mathrm{d}^{-1}(q)p \;+\; V_\mathrm{d}(q), \tag{7}$$

as the desired energy structure of the closed-loop system, where $B_\mathrm{d}(q)$ and $V_\mathrm{d}(q)$ are the inertia matrix and the desired potential energy function of the closed-loop system, respectively. Note that, choosing (7), $V_\mathrm{d}(q)$ must verify

$$q_\mathrm{d} = \operatorname{argmin}(V_\mathrm{d}(q)). \tag{8}$$

We define the desired structure of J_d and R_d in order to preserve the structure of (5) and simplify the solution of the PDEs parameterized by the chosen matrices [13]. More specifically, choosing

$$J_\mathrm{d} = \begin{bmatrix}0 & B^{-1}B_\mathrm{d}\\ -B_\mathrm{d}B^{-1} & J_2,\end{bmatrix}, \tag{9}$$

where $J_2 = -J_2^\top$ is a tuning matrix, allowing for conserving the under-actuation of the system also in the closed-loop, i.e., the control action u does not act on the variable q. On the other hand, choosing

$$R_\mathrm{d} = \begin{bmatrix}0 & 0\\ 0 & \beta HB^{-1}B_\mathrm{d} + AK_\mathrm{V}A^\top\end{bmatrix}, \tag{10}$$

where $K_\mathrm{V} > 0$ is a control gain, allowing for considering the existing damping β and adding a new one with the negative feedback.

Substituting (9) and (10) into (6) leads to the desired closed-loop dynamics

$$\begin{bmatrix}\dot{q}\\ \dot{p}\end{bmatrix} = \begin{bmatrix}0 & B^{-1}B_\mathrm{d}\\ -B_\mathrm{d}B^{-1} & J_2 - \beta HB^{-1}B_\mathrm{d} - AK_\mathrm{V}A^\top\end{bmatrix}\begin{bmatrix}\nabla_q\mathscr{H}_\mathrm{d}\\ \nabla_p\mathscr{H}_\mathrm{d}\end{bmatrix}. \tag{11}$$

As customary in PBC, we consider a controller composed of two terms $u = u_\mathrm{es} + u_\mathrm{di}$, where u_es is the energy shaping term, and u_di is the damping injection action. Equating (6) and (11) leads to

$$\begin{bmatrix}0 & I\\ -I & \beta H\end{bmatrix}\begin{bmatrix}\nabla_q\mathscr{H}\\ \nabla_p\mathscr{H}\end{bmatrix} + \begin{bmatrix}0\\ A\end{bmatrix}(u_\mathrm{es} + u_\mathrm{di}) = \begin{bmatrix}0 & B^{-1}B_\mathrm{d}\\ -B_\mathrm{d}B^{-1} & J_2 - \beta HB^{-1}B_\mathrm{d} - AK_\mathrm{V}A^\top\end{bmatrix}\begin{bmatrix}\nabla_q\mathscr{H}_\mathrm{d}\\ \nabla_p\mathscr{H}_\mathrm{d}\end{bmatrix}. \tag{12}$$

Since u_di is the negative feedback that acts on the system damping, we can define it directly as

$$u_\mathrm{di} = -K_\mathrm{V}A^\top\nabla_p\mathscr{H}_\mathrm{d}. \tag{13}$$

The energy shaping controller is found by substituting (13) in (12)

$$u_\mathrm{es} = A^*\Big(\nabla_q\mathscr{H} - B_\mathrm{d}B^{-1}\nabla_q\mathscr{H}_\mathrm{d} + J_2B_\mathrm{d}^{-1}p\Big), \tag{14}$$

where A^* is a left-inverse, for example $A^* = (A^\top A)^{-1}A^\top$. The feasibility of the control law (14) relies upon the existence of the solutions of a set of PDEs in the unknowns B_d, J_2 and V_d:

$$A^\perp\Big(\nabla_q\mathscr{H} - B_\mathrm{d}B^{-1}\nabla_q\mathscr{H}_\mathrm{d} + J_2B_\mathrm{d}^{-1}p\Big) = 0, \tag{15}$$

where $A^\perp$ is a full rank left annihilator of A.

Proposition 1: Equation (15) is solved by choosing

$$B_\mathrm{d} = K_\mathrm{B}B, \quad J_2 = 0, \tag{16}$$

and

$$V_\mathrm{d} = \frac{k}{2K_\mathrm{B}}q^\top Hq + \frac{mgh}{K_\mathrm{B}} - \frac{k}{2K_\mathrm{B}}\Big(q_0 + \frac{1}{2}q_1\Big)^2 + \frac{K_\mathrm{P}}{2}\Big[(q_0 - q_{\mathrm{d}_0}) + \frac{1}{2}(q_1 - q_{\mathrm{d}_1})\Big]^2 + \frac{k}{4K_\mathrm{B}}\Big(q_0 + \frac{1}{2}q_1\Big)^2, \tag{17}$$

where K_B and $K_\mathrm{P} \in \mathbb{R}$ are control gains.

Proof: Eq. (15) can be split into kinetic energy PDE, and potential energy PDE, obtained by dividing its kinetic and potential terms [10].

Eq. (16) solves the kinetic PDE

$$A^\perp\Big(\nabla_q(p^\top B^{-1}p) - B_\mathrm{d}B^{-1}\nabla_q(p^\top B_\mathrm{d}^{-1}p) + 2J_2B_\mathrm{d}^{-1}p\Big) = 0$$

$$A^\perp\Big(\nabla_q\big(p^\top B^{-1}p\big) - \frac{K_\mathrm{B}}{K_\mathrm{B}}\nabla_q\big(p^\top B^{-1}p\big) + 0\Big) = 0.$$

Eq. (17) solves the potential PDE

$$A^\perp\Big(\nabla_q V - B_\mathrm{d}B^{-1}\nabla_q V_\mathrm{d}\Big) = 0, \tag{18}$$

and is derived considering $V = \frac{k}{2}q^\top Hq + mgh$, evaluating $\frac{\partial V}{\partial q} = \begin{bmatrix} kq_0 + \frac{k}{2}q_1 + mg\frac{\partial h}{\partial q_0} \\ \frac{k}{2}q_0 + \frac{k}{3}q_1 + mg\frac{\partial h}{\partial q_1} \end{bmatrix}$, and defining V_d as

$$V_\mathrm{d} = \frac{k}{2K_\mathrm{B}}q^\top Hq + \frac{mgh}{K_\mathrm{B}} - \frac{k}{2K_\mathrm{B}}(q_0 + \gamma q_1)^2 + \Phi(q_0 + \gamma q_1) \tag{19}$$

where $\gamma \in \mathbb{R}$ is a parameter to be defined and $\Phi \in \mathbb{R}$ is an arbitrary differential function that we have to define to satisfy (8) for $q_\mathrm{d} = [0, 0]^\top$. We define Φ as proposed in [14]

$$\Phi(q_0 + \gamma q_1) = \frac{K_P}{2}\left[(q_0 - q_{\mathrm{d}_0}) + \gamma\left(q_1 - q_{\mathrm{d}_1}\right)\right]^2 + \frac{k}{4K_B}(q_0 + \gamma q_1)^2. \tag{20}$$

It is worth noting that (20) satisfies $\nabla_q V_\mathrm{d}(q_\mathrm{d}) = 0$.

Substituting (19) in (18) leads to

$$\begin{aligned} &A^\perp\left(\frac{\partial}{\partial q}(\frac{k}{2}q^\top Hq + mgh)\right) - A^\perp\left(K_\mathrm{B}\frac{\partial}{\partial q}(\frac{k}{2K_\mathrm{B}}q^\top Hq + \frac{mgh}{K_\mathrm{B}})\right) \\ &+ A^\perp\left(-K_\mathrm{B}\frac{\partial}{\partial q}(-\frac{k}{4K_\mathrm{B}}(q_0 + \frac{1}{2}q_1)^2)\right) \\ &+ A^\perp\left(-K_\mathrm{B}\frac{\partial}{\partial q}(\frac{K_\mathrm{P}}{2}((q_0 - q_{\mathrm{d}_0}) + \frac{1}{2}(q_1 - q_{\mathrm{d}_1}))^2)\right) = 0 \end{aligned}$$

Then, choosing $\gamma = 0.5$ solves the equation

$$A^\perp\begin{bmatrix} \frac{k}{4}(2q_0 + q_1) - \frac{K_\mathrm{B}K_\mathrm{P}}{2}(2q_0 - 2q_{\mathrm{d}_0} + q_1 - q_{\mathrm{d}_1}) \\ \frac{k}{4}\left(q_0 + \frac{1}{2}q_1\right) - \frac{K_\mathrm{B}K_\mathrm{P}}{2}\left(q_0 - q_{\mathrm{d}_0} + \frac{1}{2}q_1 - \frac{1}{2}q_{\mathrm{d}_1}\right) \end{bmatrix} = 0.$$

■

Proposition 2: The closed loop generated when applying

$$u = -K_\mathrm{B}K_\mathrm{P}\left(q_0 - q_{\mathrm{d}_0} + \frac{q_1}{2} - \frac{q_{\mathrm{d}_1}}{2}\right) + k\left(\frac{q_0}{2} + \frac{q_1}{4}\right) - \frac{K_\mathrm{V}}{K_\mathrm{B}}\left(\dot{q}_0 + \frac{\dot{q}_1}{2}\right) \tag{21}$$

to the system (5), has $(q_\mathrm{d}, \underline{0})$ as asymptotically stable equilibrium for all K_B.

Proof: Defining the Lyapunov function candidate [15] as $W = \mathscr{H}_\mathrm{d} + \mathscr{C}$, where $\mathscr{C} > 0$ is a constant such that W is positive definite [7], the time derivative of W, evaluated along the trajectories of the closed-loop system (11) is

$$\begin{aligned} \dot{W} = \dot{\mathscr{H}}_d &= \left(\nabla_q \mathscr{H}_d\right)^\top \dot{q} + \left(\nabla_p \mathscr{H}_d\right)^\top \dot{p} \\ &= \left(\nabla_q \mathscr{H}_d\right)^\top \left(K_\mathrm{B}\nabla_p \mathscr{H}_d\right) \\ &\quad + \left(\nabla_p \mathscr{H}_d\right)^\top \left(-K_\mathrm{B}\nabla_q \mathscr{H}_d - AK_\mathrm{V}A^\top \nabla_p \mathscr{H}_d - \beta HK_\mathrm{B}\nabla_p \mathscr{H}_d\right) \\ &= -\nabla_p \mathscr{H}_d^\top AK_V A^\top \nabla_p \mathscr{H}_\mathrm{d} - \nabla_p \mathscr{H}_\mathrm{d}^\top \beta HK_\mathrm{B}\nabla_p \mathscr{H}_\mathrm{d} \\ &= -\nabla_p \mathscr{H}_d^\top \left(AK_V A^\top + \beta HK_\mathrm{B}\right)\nabla_p \mathscr{H}_\mathrm{d} \;\leq\; 0 \end{aligned}$$

It is worth noting that $\dot{p} \in \mathscr{L}_\infty$, p is bounded and asymptotically converges to zero. Furthermore, substituting $p = \dot{p} = 0$ in the closed-loop equations the condition $\nabla_q V_\mathrm{d} = 0$ is obtained. Since $\nabla_q V_\mathrm{d}(q_\mathrm{d}) = 0$, according to the *Barbashin-Krasovskii* theorem, $(q_\mathrm{d}, \underline{0})$ is an asymptotically stable equilibrium. ■

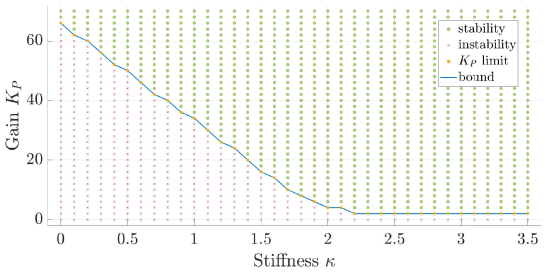

Fig. 3. Stability w.r.t. the robot stiffness: green circles represent K_P values that guarantee closed-loop stability while red crosses represent the ones for which the closed-loop is unstable.

A. Tuning of the Gains

The choice of the control gains must avoid reducing the compliance of the manipulator in a closed loop [16] and has to guarantee asymptotic stability. Writing the state equation of the SIP system

$$\begin{aligned} \dot{q} &= \dot{q} \\ \dot{p} &= B^{-1}\left[\left(-\frac{k}{2}H + \frac{k}{2}AA^\top - K_\mathrm{B}K_\mathrm{P}AA^\top\right)q - mg\frac{\partial h}{\partial q}\right] \\ &\quad - B^{-1}\left[\left(\frac{K_\mathrm{V}}{K_\mathrm{B}}AA^\top + \beta H\right)\dot{q}\right], \end{aligned} \tag{22}$$

it is possible to note that the gain of the energy-shaping is related to the stiffness of the robot k while the one of the damping injection is related to the damping β. In particular, applying Lyapunov's indirect method, we study the first dependency numerically, to show how the value of K_P depends on k.

Linearizing (22) in $[q^\top, \dot{q}^\top]^\top = [0, 0, 0, 0]^\top$ leads to

$$\begin{bmatrix} \dot{q} \\ \dot{p} \end{bmatrix} = \begin{bmatrix} 0_{2\times 2} & I \\ \mathscr{J}_1(\ddot{q}, q) & \mathscr{J}_2(\ddot{q}, \dot{q}) \end{bmatrix}_{|(0,0,0,0)} \begin{bmatrix} q \\ \dot{q} \end{bmatrix}, \tag{23}$$

where $\mathscr{J}_1(\ddot{q}, q)$ and $\mathscr{J}_2(\ddot{q}, \dot{q})$ are the Jacobian of $\ddot{q}$ w.r.t. q and the Jacobian of $\ddot{q}$ w.r.t. $\dot{q}$, respectively. We found the value of K_P for which the stability is guaranteed. Fig. 3 shows that a softer robot requires a larger gain K_P to be asymptotically stable in the studied equilibrium point.

IV. Simulation Results

In this section, the implemented IDA-PBC control is applied to the SIP to stabilize it in its vertical configuration when this is an unstable equilibrium. Then, the same swing-up problem is solved with other controllers proposed in the literature to compare our results and show the competitiveness of our method.

A. Swing-Up

Fig. 4 summarizes the results obtained from different simulation tests. We consider two different stiffness values for the SIP, i.e., $k = 1$, $k = 2$, to highlight that the required control gains for stabilization are higher the softer the robot is. Furthermore, for each value of k, three different initial positions are chosen for the SIP to show how it can be stabilized in its unstable equilibrium with the proposed IDA-PBC starting from several configurations.

Tab. I reports the values of the start configuration and the control gains for each presented test. In all tests, the desired configuration is the vertical equilibrium, i.e., $q_\mathrm{d} = [0, 0]^\top$.

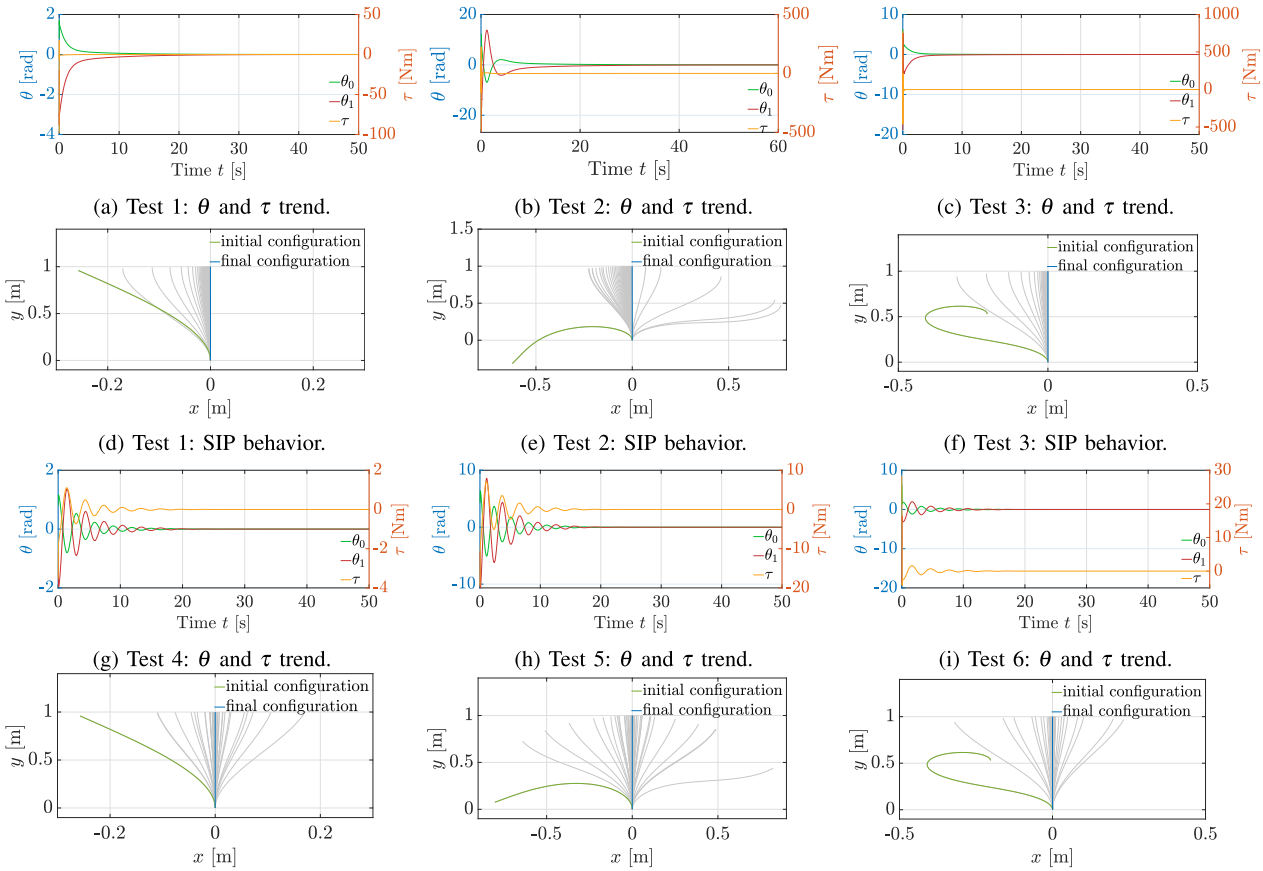

(a) Test 1: θ and τ trend. (b) Test 2: θ and τ trend. (c) Test 3: θ and τ trend.

(d) Test 1: SIP behavior. (e) Test 2: SIP behavior. (f) Test 3: SIP behavior.

(g) Test 4: θ and τ trend. (h) Test 5: θ and τ trend. (i) Test 6: θ and τ trend.

(j) Test 4: SIP behavior. (k) Test 5: SIP behavior. (l) Test 6: SIP behavior.

Fig. 4. Simulation results of IDA-PBC control. Two stiffness values, $k = 1$, $k = 2$, are considered, and for each one, three different start configurations of the SIP, for a total of six cases 1. (a), (b), (c), (g), (h), (i) report the trend of θ_0 in green, θ_1 in red, and τ in yellow for the six cases, respectively. Figs. 4(d), (e), (f), (j), (k), (l) represent respectively the robot behavior in the same six cases; the green line indicates the start configuration, the blu line the final configuration, and the grey lines the intermediate configurations.

TABLE I
TEST PARAMETERS

Test	Stiffness k	Start q		K_B	K_P	K_V
		q_0	q_1			
1 (Fig. 4a,4d)	1	$\pi/4$	$-\pi/4$	10	25	1
2 (Fig. 4b,4e)	1	$q\bar{0}_{sx}$	$q\bar{1}_{sx}$	10	25	1
3 (Fig. 4c,4f)	1	2π	-6π	10	25	1
4 (Fig. 4g,4j)	2	$\pi/4$	$-\pi/4$	10	1	0.1
5 (Fig. 4h,4k)	2	$q\bar{0}_{sx}$	$q\bar{1}_{sx}$	10	1	0.1
6 (Fig. 4i,4l)	2	2π	-6π	10	1	0.1

B. Comparison Analysis

The comparison analysis is made by solving the swing-up problem with a PD controller and with Feedback Linearization (FL), both available in the literature [3], [5].

1) PD Controller: the PD control law is a generalization for the under-actuated systems of the one derived for the continuum fully-actuated soft systems [3].

$$\tau(q_\mathrm{d}, q, \dot{q}) = A^L((kHq) + G(q)) + K_\mathrm{P} A^\top (q_\mathrm{d} - q) - K_\mathrm{D} A^\top \dot{q}$$

with A^L the left inverse of A, $K_\mathrm{P} = 3$ and $K_\mathrm{D} = 0.01$ (Fig. 5(a), 5(b)).

2) FL Control: in [5] the Author proposes a partial collocated feedback linearization by rewriting the dynamics as

$$\tilde{B}(z)\ddot{z} + \tilde{C}(z,\dot{z})\dot{z} + \tilde{G}(z) + \tilde{K}z + \tilde{D}\dot{z} = \begin{bmatrix} \tau \\ 0 \end{bmatrix},$$

where $z = [\theta_0 + \frac{1}{2}\theta_1, \frac{1}{2}\theta_0 + \frac{1}{3}\theta_1]$, $\tilde{B}(z) = H^{-1}B(H^{-1}z)H^{-1}$, $\tilde{C}(z,\dot{z}) = H^{-1}C(H^{-1}z, H^{-1}\dot{z})H^{-1}$, $\tilde{G}(z) = H^{-1}G(H^{-1}z)$, $\tilde{K} = kH^{-1}$, and $\tilde{D} = \beta H^{-1}$. The control law is

$$\tau = \left(h_1 - \left(\tilde{B}_{2,1}/\tilde{B}_{2,2}\right)h_2\right) + \left(\tilde{B}_{1,1} - \tilde{B}^2_{2,1}/\tilde{B}_{2,2}\right)u,$$

where $u = -\varphi_\mathrm{P} z_0 - \varphi_\mathrm{D}\dot{z}_0$ is an extra PD control with $\varphi_\mathrm{P} = 1$ and $\varphi_\mathrm{D} = 1$ in reported simulation (Fig. 5(c), 5(d))

C. Discussion

Simulation results for the implemented IDA-PBC demonstrate its effectiveness in addressing the swing-up problem by leveraging the energetic characteristics of the Soft Inverted Pendulum (SIP). It is important to highlight that the necessary input torque, consistent with our findings during the definition of the control law, increases not only in proportion to the deviation of the initial configuration from the desired one but also with the softness of the robot. It is also noteworthy that the robot's behavior becomes significantly more oscillatory as the parameter k increases. This behavior is attributed to the accumulation of energy within the robot, leading to pronounced oscillatory dynamics that, depending on the input torque value, may escalate into the snap phenomenon [17]. Analyzing the results of the comparisons, for which we considered only the case with $k = 1$, we can observe that the proposed controller gives smoother trends of θ_0 and θ_1 compared to those obtained with PD and FL, although with slower response times compared to PD. Evaluating the root mean squared

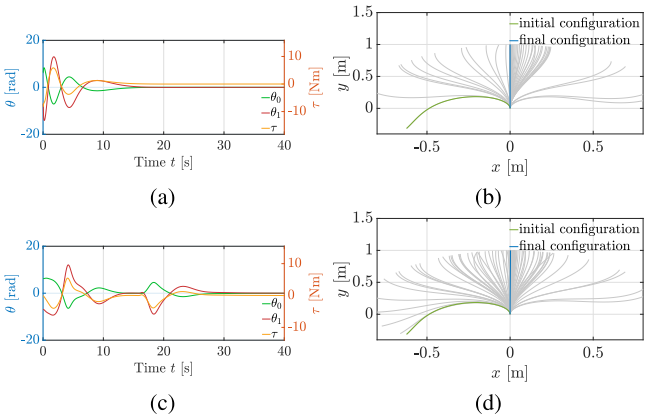

Fig. 5. Simulation results PD and FL control: the stiffness is set to 1, the start configuration is the left equilibrium for $\tau = 0$ Nm equal to $[-6.18, 6.87]^\top$ rad and the desired final configuration is $[0, 0]^\top$ rad. (a) and (c) show the trend of θ_0 in green, θ_1 in red, and τ in yellow in the case of PD and FK, respectively. Figs. 5(b) and (d) represent respectively the robot behavior in the case of PD and FL; the green line indicates the start configuration, the blu line the final configuration, and the grey lines the intermediate configurations.

error of θ_0 and θ_1 for all three cases, considering zero as the desired reference value for both variables (corresponding to the desired vertical configuration), we obtain $rmse_{\theta_0} = 1.0989$ and $rmse_{\theta_1} = 2.1263$ with IDA-PBC, $rmse_{\theta_0} = 4.6836$ and $rmse_{\theta_1} = 7.4893$ with PD, and $rmse_{\theta_0} = 3.3527$ and $rmse_{\theta_1} = 5.1856$ with FL. Moreover, given that the suggested IDA-PBC requires higher control gains when k is very small, we assessed the cost of the control action as the modulus of the integral of the input torque over time. The resulting costs, equal to 4.2764, 2.3465, and 6.7094 for IDA-PBC, PD, and FL, respectively, underscore that the overall cost incurred with our energy-based control is comparable to others, in particular, lower than that of FL. The suggested IDA-PBC has proven to be a competitive control method that, different from the two others, allows exploiting the energetic components that play a significant role in the dynamic behavior of continuum soft robots.

V. Conclusion

In the field of continuum soft robots, this research proposed a study on the soft inverted pendulum and a model-based control for the system. The objective was to realize a model-based controller to obtain highly performant soft robots. The choice of the model-based approach derived from the necessity of guaranteeing more stability and velocity in order to realize more complex tasks. The research proposed the design of an IDA-PBC to shape the energy and guarantee damping injection at the same time. The definition of the control law required the definition of the Hamiltonian function of the system and the resolution of two PDEs. It is worth noting that, the solution of PDFs does not always exist. However, with this letter, we demonstrated that a closed-form solution for both PDEs exists for the considered model. The effectiveness of the control method was demonstrated through simulations and comparisons with state-of-the-art controllers.

Future work will be devoted to extending the proposed energy-based controller to multiple models (and robots) [18], [19], [20], trajectory tracking problems, and experimental validation. Even if experimental validation remains a bottleneck for soft continuum robots, it was demonstrated that implementing actuation at the structure's tip enables good control in both regulation and tracking tasks [21]. It is reasonable to anticipate that the proposed control strategy could deliver promising results in experimental settings, considering its dependence on information about angles, which can be obtained through bend sensors, and tip actuation methods such as cable-driven systems or human-muscle-inspired single-fiber actuators. The only constraint that could be addressed is the requirement for higher torque in the case of high soft structures.

References

[1] C. D. Santina, M. Catalano, and A. Bicchi, "Soft robots," in *Encyclopedia of Robotics*. Heidelberg, Germany: Springer, Feb. 2021.
[2] D. Rus and M. T. Tolley, "Design, fabrication and control of soft robots," *Nature*, vol. 521, pp. 467–475, May 2015.
[3] C. D. Santina, C. Duriez, and D. Rus, "Model based control of soft robots: A survey of the state of the art and open challenges," *IEEE Control Syst. Mag.*, vol. 43, no. 3, pp. 30–65, Jun. 2023.
[4] W. Xiaomei, L. Yingqi, and K. Ka-Wai, "A survey for machine learning-based control of continuum robots," *Front. Robot. AI*, vol. 8, Oct. 2021, Art. no. 730330. [Online]. Available: https://www.frontiersin.org/article/10.3389/frobt.2021.730330
[5] C. D. Santina, "The soft inverted pendulum with affine curvature," in *Proc. 59th IEEE Conf. Decis. Control (CDC)*, 2020, pp. 4135–4142.
[6] R. Ortega, A. J. van der Schaft, I. Mareels, and B. Maschke, "Energy shaping control revisited," in *Advanced Topics in Nonlinear Control Systems*, A. Baños, F. Lamnabhi-Lagarrigue, and F. J. Montoya, Eds. London, U.K.: Springer, 2001, pp. 277–307.
[7] R. Ortega, A. Van der Schaft, B. Maschke, and G. Escobar, "Stabilization of port-controlled hamiltonian systems: Energy-balancing and passivation," *Automatica*, vol. 38, no. 4, pp. 585–596, 2002.
[8] A. Schaft, "Port-hamiltonian systems: An introductory survey," in *Proc. Int. Congr. Math.*, vol. 3, Jan. 2006, pp. 1339–1366.
[9] P. Borja, A. Dabiri, and C. D. Santina, "Energy-based shape regulation of soft robots with unactuated dynamics dominated by elasticity," in *Proc. IEEE 5th Int. Conf. Soft Robot. (RoboSoft)*, 2022, pp. 396–402.
[10] E. Franco, A. Casanovas, F. Baena, and A. Astolfi, "Model based adaptive control for a soft robotic manipulator," in *Proc. IEEE 58th Conf. Decis. Control (CDC)*, Dec. 2019, pp. 1019–1024.
[11] E. Franco, A. G. Casanovas, and A. Donaire, "Energy shaping control with integral action for soft continuum manipulators," *Mech. Mach. Theory*, vol. 158, Apr. 2021, Art. no. 104250.
[12] A. Van Der Schaft and D. Jeltsema, "Port-hamiltonian systems theory: An introductory overview," *Found. Trends® Syst. Control*, vol. 1, nos. 2–3, pp. 173–378, 2014.
[13] R. Ortega, A. van der Schaft, B. Maschke, and G. Escobar, "Interconnection and damping assignment passivity-based control of port-controlled hamiltonian systems," *Automatica*, vol. 38, no. 4, pp. 585–596, 2002. [Online]. Available: https://www.sciencedirect.com/science/article/pii/S0005109801002783
[14] E. Franco and A. Garriga-Casanovas, "Energy-shaping control of soft continuum manipulators with in-plane disturbances," *Int. J. Robot. Res.*, vol. 40, no. 1, Mar. 2020, Art. no. 27836492090767.
[15] B. Maschke, R. Ortega, and A. van der Schaft, "Energy-based Lyapunov functions for forced hamiltonian systems with dissipation," in *Proc. 37th IEEE Conf. Decis. Control*, vol. 4, 1998, pp. 3599–3604.
[16] C. Della Santina et al., "The quest for natural machine motion: An open platform to fast-prototyping articulated soft robots," *IEEE Robot. Autom. Mag.*, vol. 24, no. 1, pp. 48–56, Mar. 2017.
[17] F. Stoll, "Analysis of the snap phenomenon in buckled plates," *Int. J. Non-Linear Mech.*, vol. 29, no. 2, pp. 123–138, 1994. [Online]. Available: https://www.sciencedirect.com/science/article/pii/0020746294900310
[18] L. Ding et al., "Dynamic finite element modeling and simulation of soft robots," *Chin. J. Mech. Eng.*, vol. 35, no. 1, p. 24, 2022.
[19] H.-S. Chang et al., "Energy shaping control of a cyberoctopus soft arm," in *Proc. 59th IEEE Conf. Decis. Control (CDC)*, 2020, pp. 3913–3920.
[20] D. Caradonna, M. Pierallini, C. D. Santina, F. Angelini, and A. Bicchi, "Model and control of R-soft inverted pendulum," *IEEE Robot. Autom. Lett.*, vol. 9, no. 6, pp. 5102–5109, Jun. 2024.
[21] Z. J. Patterson, A. P. Sabelhaus, and C. Majidi, "Robust control of a multi-axis shape memory alloy-driven soft manipulator," *IEEE Robot. Autom. Lett.*, vol. 7, no. 2, pp. 2210–2217, Apr. 2022.

Open Access funding provided by 'Università di Pisa' within the CRUI CARE Agreement